Performance Test of a Commercial Rotational Motions Sensor

Joachim Wassermann, Susanne Lehndorfer, Heiner Igel and Ulrich Schreiber

Joachim Wassermann
Department of Earth and Environmental Sciences, LMU Munich
Theresienstrasse 41
D-80333 Munich
Germany
Tel. +4989218073962
FAX: +4989218073970
email: jowa@geophysik.uni-muenchen.de

Authors Affiliations, Addresses

Joachim Wassermann, Susanne Lehndorfer, Heiner Igel
Department of Earth and Environmental Sciences, Ludwig-Maximilians Universitaet Muenchen Theresienstrasse 41, D-80333 Munich, Germany

Ulrich Schreiber
Forschungseinrichtung Satellitengeodäsie,Technische Universitaet Muenchen,
Fundamentalstation Wettzell, Sackenriederstrasse 25, D-93444 Kötzting, GERMANY.

Performance Test of a Commercial Rotational Motions Sensor

Joachim Wassermann 1), Susanne Lehndorfer 1), Heiner Igel 1) and Ulrich Schreiber 2)

1) Department of Earth- and Environmental Sciences, LMU Muenchen, Theresienstrasse 41, D-80333 Muenchen, Germany
2) Forschungseinrichtung Satellitengeodäsie, Technische Universitaet Muenchen, Fundamentalstation Wettzell, Sackenrieder-strasse 25, D-93444 Kötzting, GERMANY.

Abstract: Only recently the application of rotational motion sensors proofed to give new ways of measuring seismic wave field properties when comparing the recorded data with seismograms of collocated traditional seismometers. The data in these test cases were produced either using sophisticated and thus expensive ring laser technology or cumbersome seismic array techniques including some restrictive assumption about the wave field. In this paper we want to test the performance of one of the first medium priced, commercial rotational motions sensor (eentec R1) by comparing its output with the aforementioned classical array derived rotational motions. The data set consists of seismic array and rotational motion measurements which were performed during a demolition blast of a 50 m high building in the city of Munich (Germany). In addition to the simple comparison of the outputs, we want to classify the performance of the two methods by comparing derived wave field properties with the result of classical f-k array analysis. The results of this experiment demonstrates, that when using array technique for estimating rotational motions much effort in site selection, array design and a priori knowledge of subsurface conditions is needed. It becomes also evident that the performance of an array and its estimated quantities depends strongly on the number of deployed seismic stations. Given the uncertainties in both the array-derived measurements and the rotation sensor transfer function it is difficult to quantify the accuracy of the rotation sensor data,

indicating the need for further extensive laboratory and field testing.

Introduction

Following the statement of Aki and Richards (2002) that a complete representation of the earth ground motion needs next to translational motions also the recording of rotations and strain, several paper demonstrate that it is possible to compute rotational motions in the far field of a seismic source using small aperture seismic arrays and derived spatial derivatives, respectively (Spudich et al., 1995; Spudich and Fletcher, 2008; Langston, 2007; Suryanto et al., 2006). Testing a geodetic ring laser for its sensitivity to rotational motions Suryanto et al. (2006) showed, that this ring laser shows equal or even superior performance in comparison to the vertical component of array derived rotational motions. The authors conclude that noise in the computed array derived rotational motions is strongly dependent on the number of stations used. Igel et al. (2007, 2005) demonstrate that using the ratio of transverse acceleration of a traditional 3C translation sensor (i.e., a seismometer) and rotational motions could lead to new techniques for measuring the apparent wave velocity and backazimuth without the need of deploying a complete seismic array.

An additional motivation for designing new rotational motion instruments originates from the inherent restrictions of array derived rotation motions. Strictly speaking its formal derivation is only valid assuming a linear gradient of the wavefield, i.e., mainly in its far field and without further pollution of the seismometers by tilt signals, assumptions which may not always be fulfilled in the real world. In the light of the increasing interest in measuring rotational motions particularly in connection with earthquake engineering and strong ground motion problems it is important to investigate thoroughly the performance of rotation sensors, particularly those that can be deployed in the field. Here we report on a field test of the eentec R1 three component rotation sensor and estimate its performance by comparing with rotational motions derived from a seismic array as well as classical seismic array analysis. Seismic energy was generated by a collapsing building initiated by explosions.

Experiment Setup and Discussion

The data used in this study consists of a seismic seven element array with an aperture of 70 m and mean station distance of 20 m (Fig. 1). In the center of the array an eentec R1 rotational motions sensor is collocated to a Streckeisen STS-2 broadband sensor (see Fig 1, station 01) forming the core elements of the experiment. The sampling rate is set to 200 Hz for all used instruments. The distance from the eentec R1 location (station 01), the reference point of the array, to the blast site (black square in Fig. 1) is approximately 250 m with a backazimuth of 280°. The building and the array are situated both on a uniform thick layer of glacial rubble making differences in site amplification of array stations rather unrealistic. The blast itself consists of 150 kg explosives fired sequentially to reduce ground shaking. The blasted building, however, was hoped to produce high portion of rotational motions and tilt as it was going to fulfill a twisted motion while collapsing.

Following Spudich and Fletcher (2008) we first compute the frequency band for which the error of the array derived rotational motion stays below 10%. The error is caused by deviations from the assumed linear gradient of the wavefield and is depending strongly on the aperture of the array. As a first approximation, we assume a wave speed of 1000m/s as an initial guess. Using the aperture of 70m, which was chosen to apply also classical f-k array analysis, we estimate the upper corner frequency to be at 3.5 Hz. Reducing the arrays aperture to 35m by reducing the number of stations, will therefore result in a corner frequency of 7 Hz. In this context it is important to note, that the main seismic energy during the blast and the following collapse was radiated in narrow frequency band around 6 Hz.

The lower frequency limit was chosen because of mixing broadband (Streckeisen STS-2 at 01, 02, 03) and short period (1 Hz - MarkL4/3C at stations 05,06; Lennartz Le3Dlite at stations 07, 08) seismometers in the experiment. Although all seismograms are corrected for the instrument transfer function down to 0.5 Hz before computing spatial derivatives, the frequency limit was set to 1 Hz and 0.8 Hz, respectively, in order to further suppress possible phase shifts caused by erroneous transfer functions. It can be shown that uncertainties in the transfer function have a strong influence especially in the vicinity of the corner (eigen) frequency of an instrument. This may cause problems in the rotational motion seismograms, which we will discuss later in more detail. In Fig. 2, data records of all directly comparable measurements (transverse acceleration, rotational motions and array derived rotations in its vertical component) are shown following the initial blast in two different frequency bands. In order to evaluate the influence of the bandwidth and number of used stations for the following comparison between different sensors and sensor configurations, we filter the data with a zero phase bandpass between 0.8 to 5 Hz and 1 to 8 Hz, respectively. While the first bandpass (Fig2.a-d) is at least nearby the optimum frequency vs. aperture relationship given by Spudich and Fletcher (2008), the second bandpass (Fig2.e-h) includes the main energy peak of radiated frequencies. It becomes immediately apparent, that the eentec R1 sensors has a larger amount of noise present in the lower frequency range. Additionally, the reduced similarity between the array derived rotational motions and the transverse acceleration in the 0.8 - 5 Hz frequency band in comparison with the corresponding traces for the 1 - 8 Hz case is remarkable. The lower performance is visible even when only four stations are used. This may reflect problems in computing array derived rotational motions when a significant portion of the recorded signal contains uncorrelated noise.

The next step is to compare array-derived rotational motions,computed using the method proposed by Spudich et al. (1995) with signals recorded by the R1 sensor.Following the statement just made, we perform this analysis in the frequency band between 1 - 8 Hz but using different array sizes. This we do although we may violate the estimation made by Spudich and Fletcher (2008) at least at some points. The comparison itself shows surprisingly good agreement (Fig. 3, Fig. 4, Fig. 5) in case of rotational signals around vertical (Z) and north (N) axes in most of the cases. Why this good match in the wave forms can not be seen in the east (E) components is still unclear (see Fig. 5 for the seven element array). If scattering is the main source of error for this component (E component is corresponding to twisting motion perpendicular to the source receiver axis, see Fig. 1) it is still unclear why the rotational motions sensor is more sensitive to this scattering waves than the array stations. Possibly the array assumption of correlated signals is violated and therefore these scattered waves are suppressed. Fig. 3, 4,and 5 also confirm the statement of Suryanto et al. (2006) that the number of used stations for computing spatial derivatives significantly changes the result. Especially the amplitudes change dramatically when increasing the number of array elements. Assuming a correct gain of the eentec R1 sensor, the seven element array shows a nearly perfect fit in amplitude (Fig. 5), while the five element array overestimates the rotational motion amplitudes by a factor of 30% (Fig. 4).

Focusing on details also differences between R1 and array derived rotation become apparent. The array-derived rotational motions show a significant phase shift especially in its N-component compared to the R1 signals (Fig. 3, 4, 5). Phase shifts are present for thefour, five and the seven sensor array, respectively, but seem to be more pronounced for the four and seven sensor array (Fig. 3,5). Even worse, the phase shift is not constant during the complete recording. Possible reasons for the phase misalignment could either be the always present noise or problems with the sensor calibrations or both. The first seems to be reasonable as the recording site was within a city with heavy traffic in its direct vicinity. However, even as the instrument correction procedure applied to the raw data should reduce possible influences of erroneous transfer functions, phase shifts as possible cause of not precisely calibrated sensors are a well known problem. As phase and amplitude mismatches are worse using the four element array, which is more or less consistent with lower error rates according to Spudich and Fletcher (2008) as well as seven element array, which includes two older seismometer of the same type (Mark L4-3C 1Hz), we restrict our further analysis to the comparison with the five element array data. This may lead to wrong velocity estimations (Igel et al., 2005, 2007) but should give at least stable results.

The performance tests presented so far were done by comparing two different ways of measuring rotational motions for which the errors are only partially known. On the one hand, the transfer function of the eentec R1 sensor, its temporal stability, cross talk between components and possible influence of translational motion on the sensors is still a matter of debate. On the other hand, assumptions needed to justify array-derived rotational motion, i.e. uniform spatial gradient, size of the array vs. curvature of the gradient (Spudich and Fletcher, 2008) and tilt (rotational) free recordings of translational motions may not be fulfilled in real world applications.

In order to test the overall quality of the two ways to measure rotational motions, we compare the results of standard f-k seismic array techniques: apparent velocity, backazimuth, semblance (see e.g., Kvaerna and Ringdahl, 1986) with the parameter computed following the procedure of Igel et al. (2005, 2007): maximum cross-correlation in a sliding window of rotational motions with transverse acceleration, backazimuth value depending on the maximum cross-correlation when probing the correlation for different azimuth values and the apparent velocity computed by the ratio of transverse acceleration (with respect to maximizing the cross-correlation) versus rotational motions (Fig. 6).

Even as the array to source distance is within just several wavelengths at 6 Hz and the assumption of plane wave incidence may not be fully correct, Fig. 6 shows clearly the advantage of using classical seismic array technique: the suppression of incoherent noise. While variations in time of the maximum of cross-correlation coefficients and semblance looks quite similar, the results for apparent velocity and backazimuth deviates strongly for both R1 and array derived rotations. Deviations in the apparent velocities can be quite naturally explained up to some degree by the different sensitivity of the methods to different wave types, i.e. Rayleigh waves in case of f-k analysis and Love waves in case of transverse acceleration vs. rotational motion ratio. However, the large deviations in the backazimuth must be explained differently. Again noise may play an important role in erroneous estimation. Another possible reason is a mis-orientation of the translation sensor. A misalignment of more than 30°, however, as seen in Fig. 6 for both methods seems not very reasonable.

In summary, the eentec R1 sensor seems to give reasonable results at least for the higher frequency portions of the signals analyzed. The experiment clearly shows problems and difficulties when using seismic arrays for recording rotational motions. Next to differences in site responses, noise seems to play a dominant role in the quality of the estimations. A larger number of sensor will suppress present noise and therefore increase the reliability of the measurement even though the assumption of a uniform gradient may be violated.

On the other hand, doubt remains about the quality of the calibration of the eentec R1 sensor especially in the lower (< 1 Hz) frequency range. Therefore the sensor should undergo more careful long term tests regarding stability and contamination by translational motions. A possible new application which combines advantages of both techniques would be to collocate a seismic array with the same number of rotational sensors in order to reduce noise effects on the different sensor types.

Data and Resources

All data used in this study were provided by the Geophysics section and the Geophysical Observatory of the Ludwig-Maximilians University Munich. The measurements were performed using equipment of the Geophysical Observatory and the Seismological Central Observatory Graefenberg (BGR).

Acknowledgments. We are grateful to H. Blachnitzky for the allowance to measure the blast in its "near field". Comments and corrections made by Paul Spudich are highly appreciated and significantly improved the manuscript. Furthermore, we would like to express our thanks to S. Egdorf and W. Bauer for their technical support and assistance even on short notice. Many thanks also to E. Wetzig from Graefenberg Array (BGR) for borrowing two of the deployed broadband sensors.

References

Aki, K. and P.G. Richards, (2002). Quantitative Seismology, 2nd Edition, University Science Books.

Igel, H., A. Cochard, J. Wassermann, A. Flaws, U. Schreiber, A. Velikoseltsev, and N. Pham Dinh (2007). Broad-band observations of earthquake-induced rotational ground motions, Geophysical Journal International, 168(1), 182-197, doi:10.1111/j.1365-246X.2006.03146.x.

Igel, H., U. Schreiber, A. Flaws, B. Schuberth, A. Velikoseltsev, and A. Cochard (2005), Rotational motions induced by the M8.1 Tokachi-oki earthquake, September 25, 2003, Geophys. Res. Lett., 32, L08309, doi:10.1029/2004GL022336.

Langston, C.A, (2007). Spatial Gradient Analysis for Linear Seismic Arrays, B.S.S.A., v. 97, no. 1B, p. 265-280, DOI: 10.1785/0120060100

Kvaerna, T., and F. Ringdahl, (1986). Stability of various f-k estimation techniques, in: Semi-annual Technical Summary, 1 October 1985 - 31 March 1986, NORSAR Scientific Report, 1-86/87, Kjeller, Norway, pp. 29-40.

Spudich, P., L. K. Steck, M. Hellweg, J. B. Fletcher, and L. M. Baker (1995), Transient stresses at Parkfield, California, produced by the M 7.4 Landers earthquake of June 28, 1992: Observations from the UPSAR dense seismograph array, J. Geophys. Res., 100(B1), 675–690.

Spudich, P, and J. B. Fletcher, (2008). Observation and prediction of dynamic ground strains, tilts, and torsions caused by the M6.0 2004 Parkfield, California, earthquake and aftershocks derived from UPSAR array observations, B.S.S.A, accept. for publication.

Suryanto, W., J. Wassermann, H. Igel, A. Cochard, D. Vollmer, F. Scherbaum, A. Velikoseltsev, and U. Schreiber (2006), First comparison of seismic array derived rotations with direct ring laser measurements of rotational ground motion, Bull. Seism. Soc. Am., 96(6), 2059-2071, doi:10.1785/0120060004.

Figure 1: Seismic array setup used and relative location of demolition blast indicated by a square. The location of the seismometers are indicated by black triangles. At station 01 a Streckeisen STS-2 broadband seismometer is colocated with the eentec R1 sensor (gray circle). 02,03 are additional sites of STS-2 broadband seismometers, 04-08 mark the location of short period (1 Hz) sensors. The inset gives an impression about the size of the building and the distance towards the array, respectively. The black arrow indicates the viewing direction of the photo (courtesy S.Egdorf).

Figure 2: Estimated transverse acceleration, using station 01 (STS-2) and the buildings backazimuth, R1 Vertical component output and array derived rotations using a four (01,03,07,08) and 7 (01,02,03,05,06,07,08) element array in different frequency bands. (a-d) represent the recorded signals in a bandpass of 0.8 - 5 Hz, while (e-h) show the same quantities but in a frequency band 1 - 8 Hz including the dominant frequency at 6 Hz.

Figure 3: Direct comparison of between R1 (black) and four element array (01,03,07,08 - see Fig. 1) derived rotational motion (gray) inall components. A pronounced mismatch in the amplitude and phase is visible.

Figure 4: Same as in Figure 3 but comparing R1 (black) Z and fiveelement array (01,02,03,07,08 - see Fig. 1) output (gray). While the amplitude still deviates, the phase match is nearly perfect in the Z component..

Figure 5: Same as in Figure 3 but comparing R1 (black) Z and seven element array (01,02,03,05,06,07,08) output (gray). While the amplitude now fits perfectly, the phase mismatch is increasing.

Figure 6: Comparison between standard f-k array analysis output and parameters computed using rotational motions recordings. Semblance, logarithmic beam power, apparent velocity and backazimuth are shown using a 0.68 s sliding window in a frequency band between 1 - 8 Hz. Only values with a semblance larger than 0.6 are shown. Maximum of cross-correlation coefficient computed in a 0.68 s sliding window between Z-component of the R1 sensor and transverse acceleration (T-axis) of the colocated seismometer, apparent velocity estimated by the ratio between acceleration and rotational motions and backazimuth. All estimates are computed while probing the optimal rotation of the horizontal seismometer components with respect to maximization of the cross correlation coefficient with time lag zero.

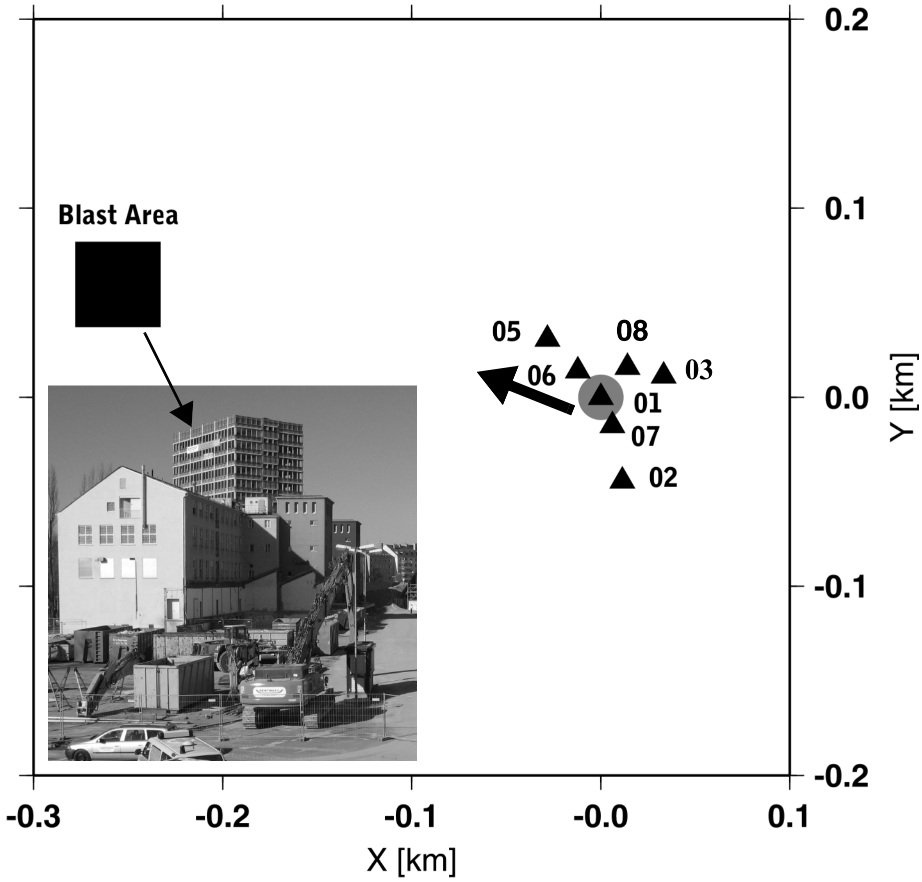

Figure 1

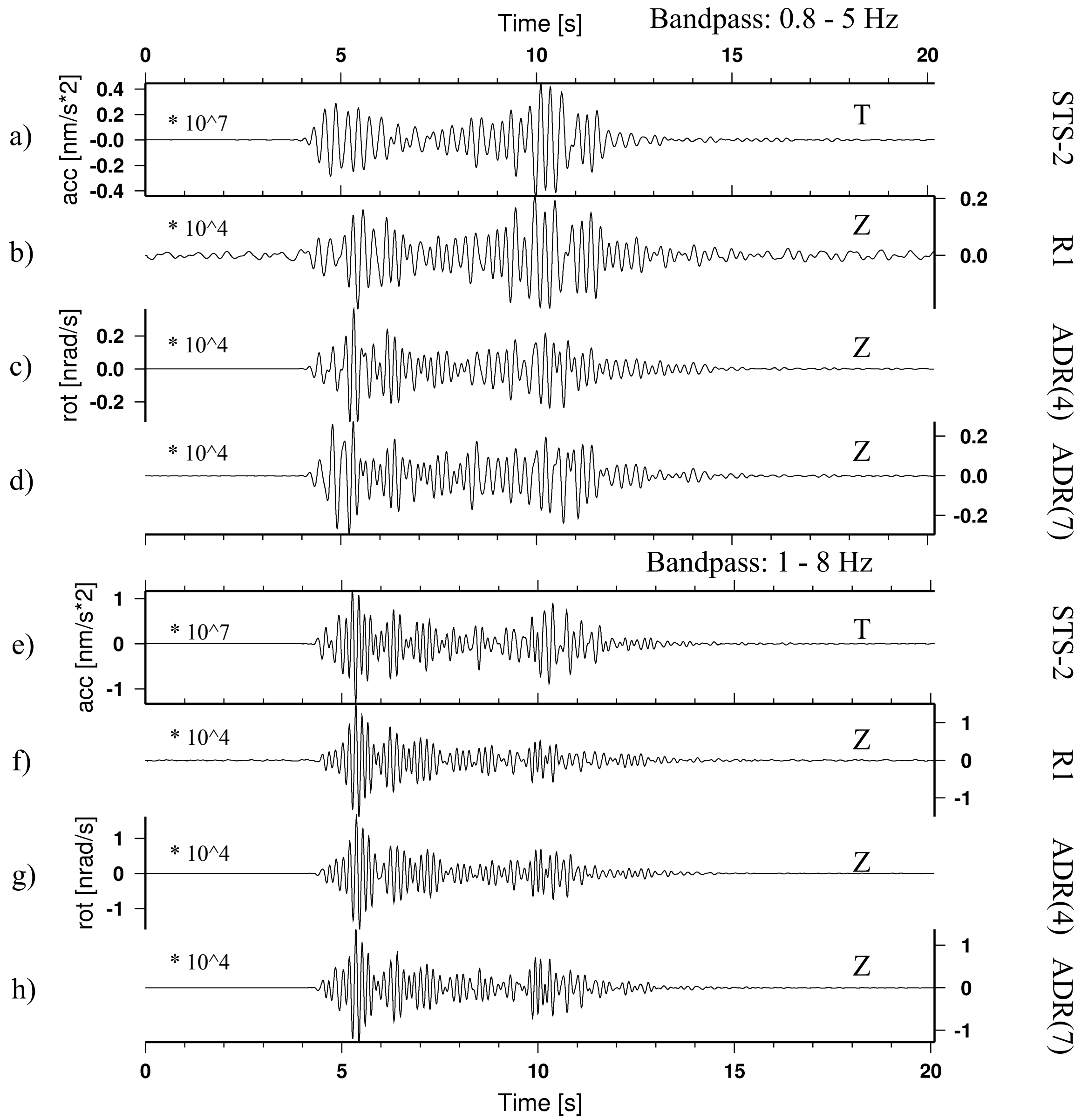
Time [s]
Bandpass: 0.8 - 5 Hz
0
5
10
15
20
a)
acc [nm/s*2]
0.4
0.2
-0.0
-0.2
-0.4
* 10^7
T
STS-2
b)
* 10^4
Z
0.2
0.0
R1
c)
rot [nrad/s]
0.2
0.0
-0.2
* 10^4
Z
ADR(4)
d)
* 10^4
Z
0.2
0.0
-0.2
ADR(7)
Bandpass: 1 - 8 Hz
e)
acc [nm/s*2]
1
0
-1
* 10^7
T
STS-2
f)
* 10^4
Z
1
0
-1
R1
g)
rot [nrad/s]
1
0
-1
* 10^4
Z
ADR(4)
h)
* 10^4
Z
1
0
-1
ADR(7)
0
5
10
15
20
Time [s]

Figure 2

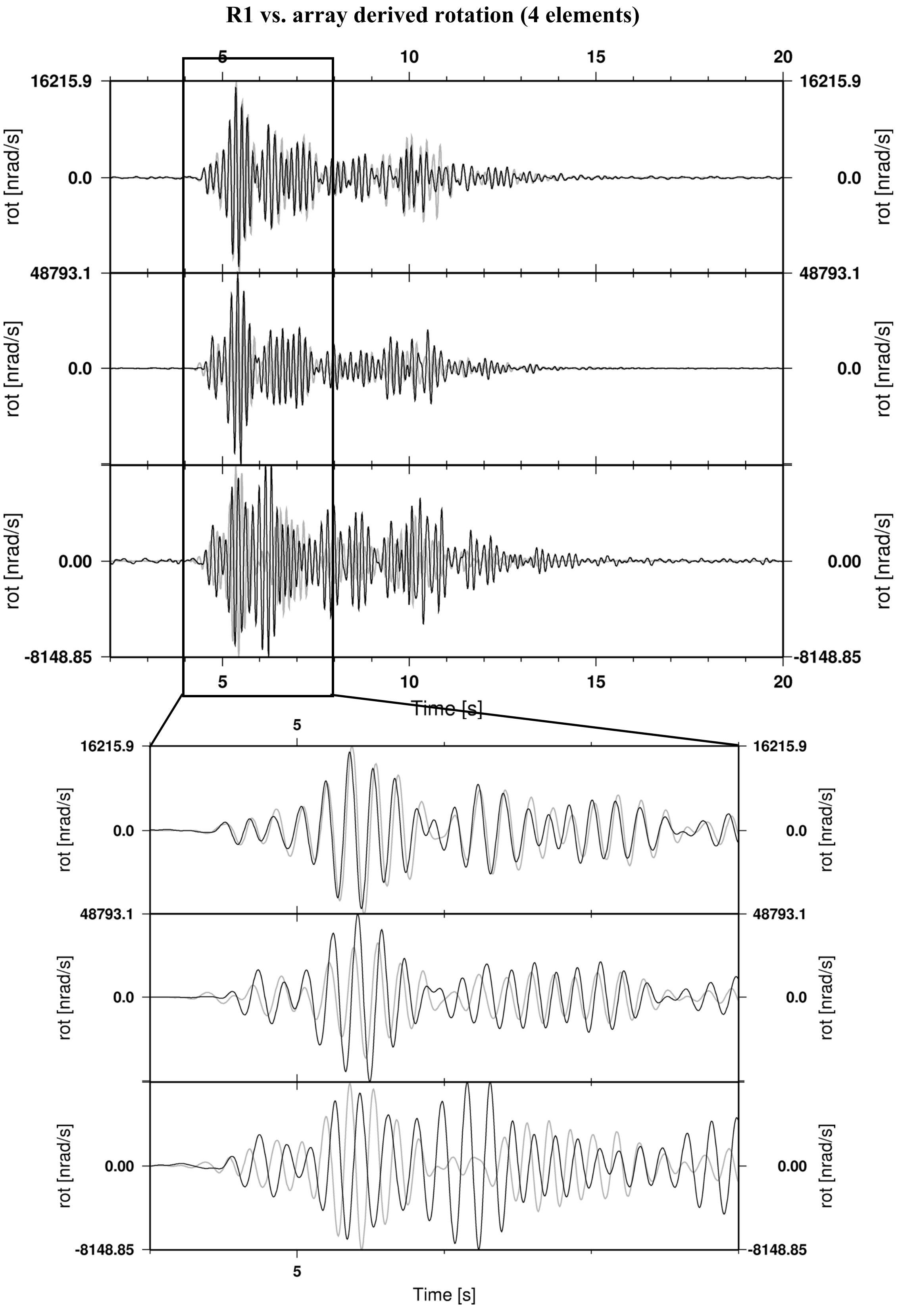
R1 vs. array derived rotation (4 elements)
5
10
15
20
16215.9
0.0
48793.1
0.00
-8148.85
rot [nrad/s]
Time [s]

Figure 3

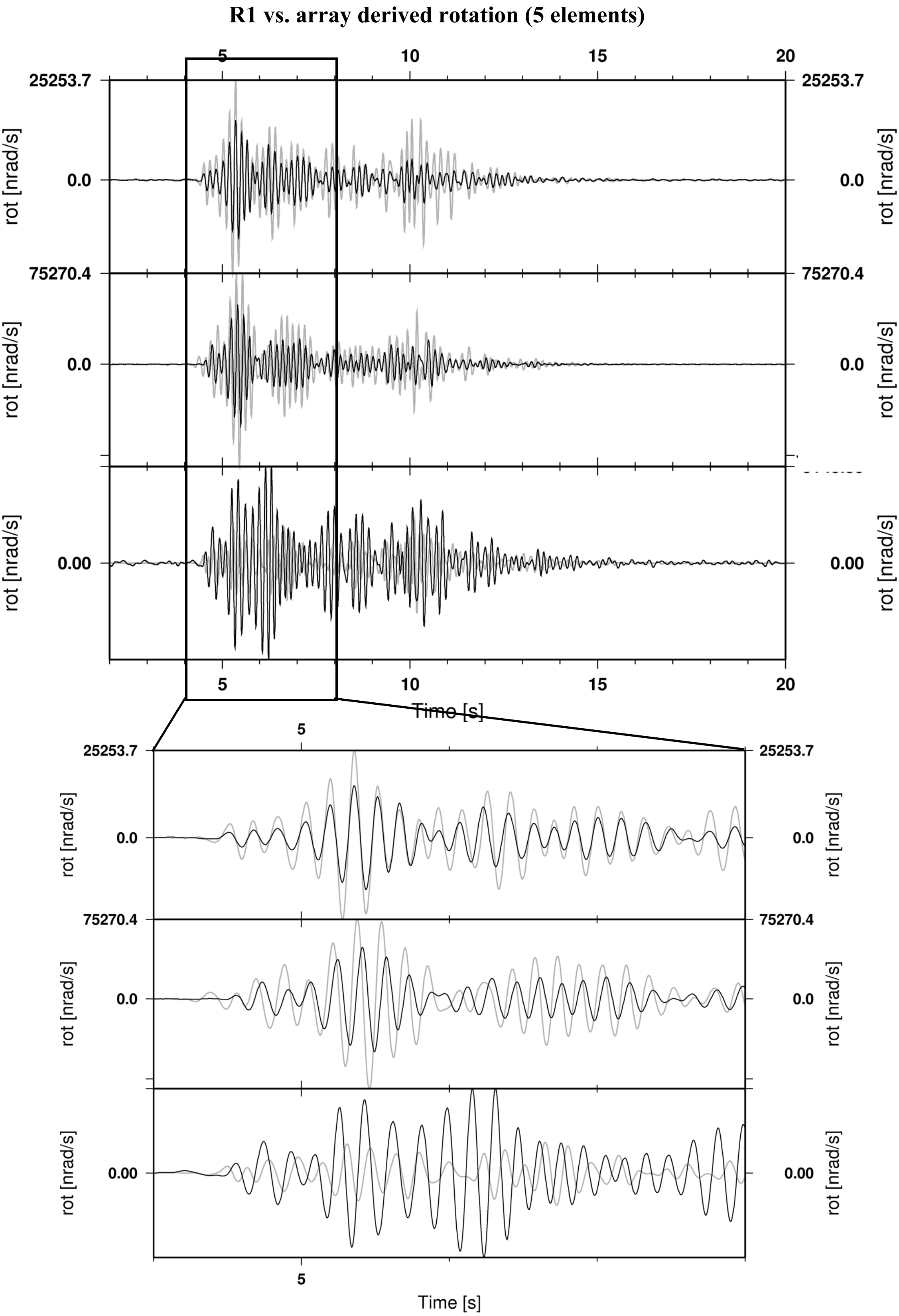
R1 vs. array derived rotation (5 elements)
5
10
15
20
25253.7
25253.7
rot [nrad/s]
0.0
0.0
75270.4
75270.4
0.00
0.00
Time [s]
5
25253.7
25253.7
0.0
0.0
75270.4
75270.4
0.0
0.0
0.00
0.00
5
Time [s]

Figure 4

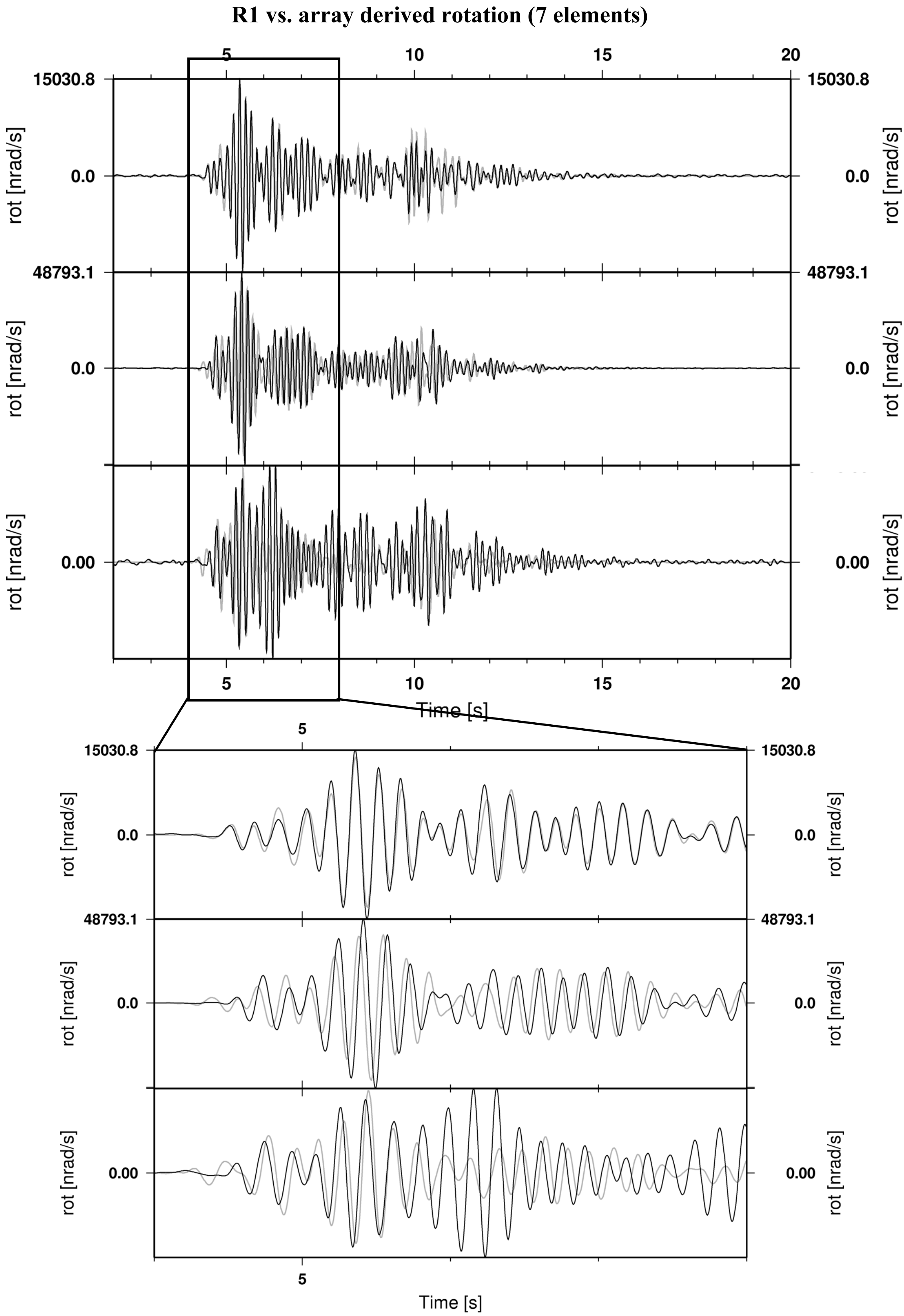
R1 vs. array derived rotation (7 elements)
5
10
15
20
15030.8
0.0
48793.1
0.00
rot [nrad/s]
Time [s]

Figure 5

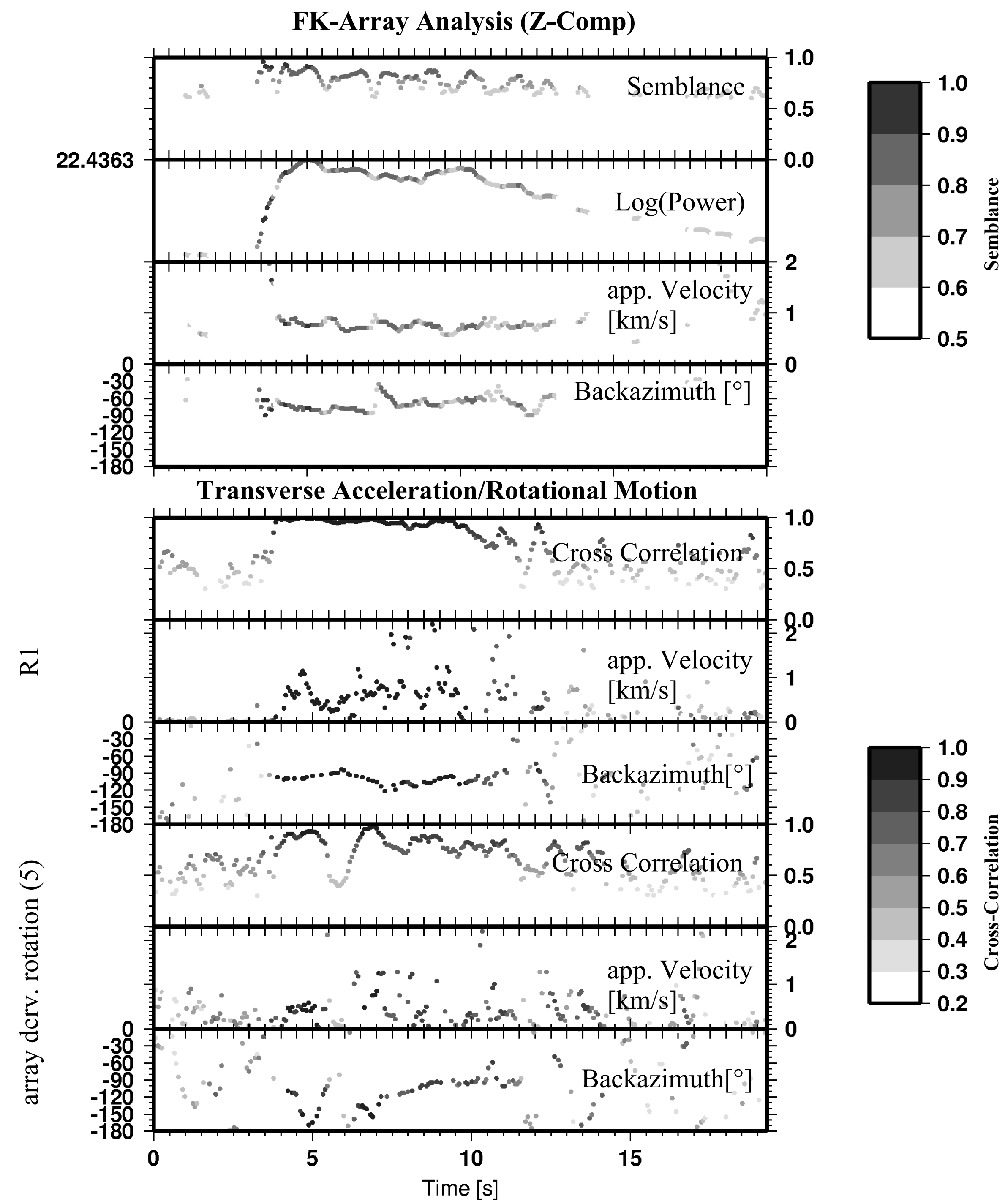

FK-Array Analysis (Z-Comp)
Semblance
Log(Power)
app. Velocity [km/s]
Backazimuth [°]
22.4363
Transverse Acceleration/Rotational Motion
Cross Correlation
R1
array derv. rotation (5)
Time [s]
Semblance
Cross-Correlation

Figure 6